

# A Network-Based Meta-Population Approach to Model Rift Valley Fever Epidemics

Ling Xue<sup>a,\*</sup>, H. Morgan Scott<sup>b</sup>, Caterina Scoglio<sup>a</sup>

<sup>a</sup>*Department of Electrical & Computer Engineering,  
Kansas State University, U.S. 66506*

<sup>b</sup>*Department of Diagnostic Medicine,  
Kansas State University, U.S. 66506*

---

## Abstract

Rift Valley Fever virus (RVFv) has been expanding its geographical distribution with important implications for both human and animal health. The emergence of Rift Valley Fever (RVF) in the Middle East, and its continuing presence in many areas of Africa, has negatively impacted both medical and veterinary morbidity, mortality, and economic endpoints. Furthermore, worldwide attention should be directed towards the broader infection dynamics of RVFv, since suitable host, vector and environmental conditions for additional epidemics likely exist on other continents; including Asia, Europe and the Americas. We extend a compartmentalized ordinary differential equation model of RVF to assess disease spread in both time and in space; with the latter driven as a function of contact networks. Four species are included in the model; namely, humans and livestock hosts, and two species of vector mosquitoes. The model is based on weighted contact networks, where nodes of the networks represent geographical regions and the weights represent the level of contact between regional pairings for each set of species. We have tested, calibrated, and evaluated the model using data from the recent (2010) RVF outbreak in South Africa as case study; mapping the epidemic spread within and among three South African provinces. An extensive set of simulation results shows the potential of the proposed approach for accurately modeling the RVF spreading process in additional regions of the world.

## Keywords:

Networks, Meta-population, Deterministic model, Rift Valley fever (RVF)

---

## 1. Introduction

Rift Valley Fever (RVF) is a viral zoonosis with enormous health and economic impacts on domestic animals and humans [28], in countries where the disease is endemic and in others where sporadic epidemics and epizootics have occurred. RVF virus (RVFv) is generally distributed through regions of eastern and southern Africa where sheep and cattle also are present [35]. The disease causes high mortality and abortion in domestic animals. It also causes morbidity (ranging

---

\*Corresponding Author

*Email addresses:* lxue@ksu.edu (Ling Xue), hmscott@vet.k-state.edu (H. Morgan Scott), caterina@k-state.edu (Caterina Scoglio)

*Preprint submitted to Elsevier*

*January 13, 2019*

from nondescript fever to meningo-encephalitis and hemorrhagic disease) and mortality (with case fatality rates of 0.2 – 5%) in humans [28]. Recurring outbreaks of RVF in Africa cost lives and adversely affect the health of both livestock and humans; often resulting in great economic losses. The main economic losses of RVF in livestock arise due to abortion and mortality, which tends to be higher in young animals [14, 35], and bans on livestock exports during an epidemic [14, 8].

The RVF virus (RVFv) was first identified in 1931. It was first isolated from the blood of a newborn lamb and later from the blood of adult sheep and cattle [32, 8]. *Aedes* and *Culex* spp. of mosquitoes are believed to be the main arthropod vectors [12] while domestic ruminants and humans are among the mammalian hosts demonstrated to amplify RVFv [25]. Of particular importance to the ecology and epidemiology of the disease, the RVFv can be transferred vertically from females to their eggs in some species of the *Aedes* mosquitoes [20, 29]. The disease has been shown to be endemic in semi-arid zones, such as northern Senegal [36, 12, 30], and RVF epidemics often appears at 5-to-15 year cycles [30]. An outbreak in South Africa in 1951 was estimated to have infected 20,000 people and killed 100,000 sheep and cattle [19, 33]. In Egypt in 1977, there were 18,000 human cases with 698 deaths resulting from the disease [19, 33]. In 1997 – 98 Kenya experienced the largest recorded outbreak with 89000 human cases and 478 death. The first recorded outbreak outside of Africa occurred in the Arabian peninsula in 2000 – 2001 and caused 683 human cases and 95 deaths [23]. Tanzania and Somalia reported 1000 human cases and 300 deaths from an outbreak that was associated with above-normal rainfall in the region in 2006 – 2007 [23]. In 2010, to date a larger-than-normal number of human cases and deaths has been reported in South Africa [24]; all of these examples confirm that humans are also at high risk of morbidity and mortality. While RVF is endemic in Africa, it also represents a threat to Europe and Western hemispheres [12, 20]. As noted earlier, RVF has already spread outside Africa, to Yemen and Saudi Arabia [12, 18]. The recent outbreaks of RVF in Kenya and neighboring Somalia, the United Republic of Tanzania, and Sudan underscore the ability of the virus to kill human and other animal hosts [25, 18, 32, 16]. The species of vectors that are capable of transmitting RVFv have a wide global distribution [22] and there is therefore a distinct possibility for the virus to spread out of its currently expanding geographic range [14]. A pathways analysis [25] has shown that the RVF virus might be introduced into the United States in several different ways [25, 26] and that analysis identified several regions of the United States that are most susceptible to RVFv introduction. It is therefore desirable to develop effective models to better understand the potential dynamics of RVF in heretofore unaffected regions and then develop efficient mitigation strategies in case this virus appears in the Western hemisphere [20]. Such preparedness can help avoid a rapid spread of the virus throughout North America, as happened with the West Nile virus during the last decade [12, 20].

A Rift Valley fever (RVF) disease risk mapping mode was developed by [5]. The authors observed sea surface temperature (SST) patterns, cloud cover, rainfall, and ecological indicators (primarily vegetation) via satellite data to evaluate different aspects of climate variability and their relationships to disease outbreaks in Africa and the Middle East [7, 6]. The researchers successfully predicted areas where outbreaks of RVF in humans and animals were expected using climate data for the Horn of Africa from December 2006 to May 2007. These predictions were subsequently confirmed. The authors were able to provided a 2 to 6 week period of warning for jurisdictions in the Horn of Africa in order to facilitate early disease outbreak response and control activities. Theirs was the first prospective prediction of a RVF outbreak as far as we know [5]. A very innovative ordinary differential equation (ODE) mathematical model was developed by [20]. The model is both an individual-based and deterministic model. The authors analyzed

the stability of the model and tested the importance of the model parameters. However, neither human population parameters nor spatial (or, network) aspects are explicitly incorporated in the model.

RVFv has been documented to be spread by wind [33]. Wind dispersal of mosquitoes has changed geographic distribution and accelerated the spread of RVFv to new geographic areas [25]. Some locations can become secondary epidemic sites after the virus has been introduced (especially in irrigated areas, e.g. Gazeera in Sudan or rice valleys in the center of Madagascar) [30]. Livestock trade and transport also can affect the geographic distribution of Rift Valley fever [12]. One critical objective in developing effective models is to determine the major factors involved in the disease spreading process.

In this paper, we present a novel model incorporating *Aedes* and *Culex* mosquito vector, and livestock and human host populations. Our model is based on weighted contact networks, where nodes of the networks represent geographical regions and weights represent the level of contact between regional pairs for each vector or host species. Environmental factors such as rainfall, temperature, wind and evaporation are incorporated into the model. For each subpopulation, a set of ordinary differential equations describes the dynamics of the population in a specific geographical location, and the transitions among the different compartments, after contracting the virus.

We test, calibrate, and evaluate the model using the recent 2010 RVF outbreak in South Africa as a case study, mapping the epidemic spread in three South African provinces: Free State, Northern Cape, and Eastern Cape. An extensive set of simulation results shows the potential of the proposed approach to accurately describe the spatial-temporal evolution of RVF epidemics.

The paper is organized as follows: 1) in Sec. 2, we describe our meta-population mathematical model, 2) in Sec. 3, we introduce the case study using outbreak data from South Africa, 2010 3), in Sec. 4, we calibrate a number of parameters and analyze the sensitivity of the model to the parameters, 4) in Sec. 5, we analyze the simulation results, and 5) finally, in Sec. 6, we conclude and discuss our work.

## 2. The mathematical model

We constructed a mathematical model based on network graphs, and use flow diagrams to describe the principle of the model.

### 2.1. Flow diagrams of the model

A compartmentalized ordinary differential equation model was based on a weighted network. The model includes two populations of mosquitoes, one population of livestock and one population of humans. The principle of local transmission is shown in Figure 1(a). Infectious *Aedes* mosquitoes can not only transmit RVFv to susceptible livestock and humans but also to their own eggs [20, 29]. *Culex* mosquitoes acquire the virus during blood meals on an infected animal and then amplify the transmission of RVFv [32]. Direct ruminant-to-human contact is the major (though not only) way for humans to acquire the infection [5, 17]. Accidental RVFv infections have been recorded in laboratory staff handling blood and tissue from infected animals [5]. Most domestic animals and fewer humans are infected due to the bites of mosquitoes [32]. Usually, humans are thought of as dead end hosts that do not contribute significantly to propagation of the epidemic [12]. There has been no direct human-to-human transmission of RVFv in field conditions recorded thus far [25]. We assume that the mosquitoes won't spontaneously recover once

they become infectious [20]. Livestock and humans can either perish from the infection or else recover [20]. All four species have a specified incubation period [32]. We use an “S-E-I” compartmental model in which individuals are either in a susceptible (S) state, an exposed (E) state, or an infected state (I) for both *Aedes* and *Culex* mosquitoes and an “S-E-I-R” compartmental model in which individuals are either in a susceptible (S) state, an exposed (E) state, an infected state (I), or a recovered (R) state for both livestock and human populations. Transmission among vector and host populations in different locations is shown in Figure 1(b) as an example. Each node represents the centroid of a province in this model. All four species are assumed to be able to migrate. The infected mosquitoes in each location will travel with wind to other locations and transmit the disease to susceptible livestock or humans in other locations. We assume that mosquitoes and livestock will not return to their original province whereas humans are permitted to return after traveling. The first number or letter of the subscript represents the species,  $x = 1$  for *Aedes*,  $x = 2$  for livestock,  $x = 3$  for *Culex* and  $x = 4$  for humans. The second letter of the subscript represents the location. We assume that the two species of mosquitoes will not recover or die from the disease [20].

## 2.2. Differential equations

The *Aedes* spp. and *Culex* spp. mosquitoes in location  $i$  ( $i = 1, 2, 3, \dots, n$ ), are distributed among susceptible  $S_{ai}$ , exposed  $E_{ai}$  and infected  $I_{ai}$  compartments. The subscript  $a = 1$  denotes *Aedes* spp. and  $a = 3$  denotes *Culex* spp. The size of each adult mosquito population in location  $i$  is  $N_{1i} = S_{1i} + E_{1i} + I_{1i}$  for *Aedes* mosquitoes and  $N_{3i} = S_{3i} + E_{3i} + I_{3i}$  for *Culex* mosquitoes. The livestock and human hosts contain susceptible  $S_{bi}$ , exposed  $E_{bi}$ , infected  $I_{bi}$  and recovered  $R_{bi}$  individuals. The subscript  $b = 2$  and  $b = 4$  denote livestock and humans respectively. The size of host populations in location  $i$  is  $N_{2i} = S_{2i} + E_{2i} + I_{2i} + R_{2i}$  for livestock hosts and  $N_{4i} = S_{4i} + E_{4i} + I_{4i} + R_{4i}$  for human hosts. The four populations are modeled with a specified carrying capacity  $K_1, K_2, K_3, K_4$  respectively. The weighted links connecting the nodes are characterized by the movements of the four species between all the compartments except for infected livestock.

The systems of ordinary differential equations (ODEs) for location  $i$  are given as follows:

### 2.2.1. *Aedes* mosquito vectors

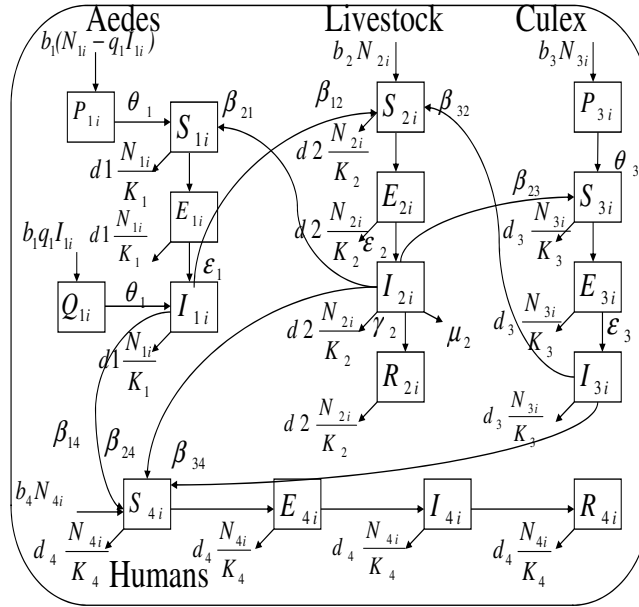
$$\frac{dP_{1i}}{dt} = b_1(N_{1i} - q_1 I_{1i}) - \theta_1 P_{1i} \quad (1)$$

$$\frac{dQ_{1i}}{dt} = b_1 q_1 I_{1i} - \theta_1 Q_{1i} \quad (2)$$

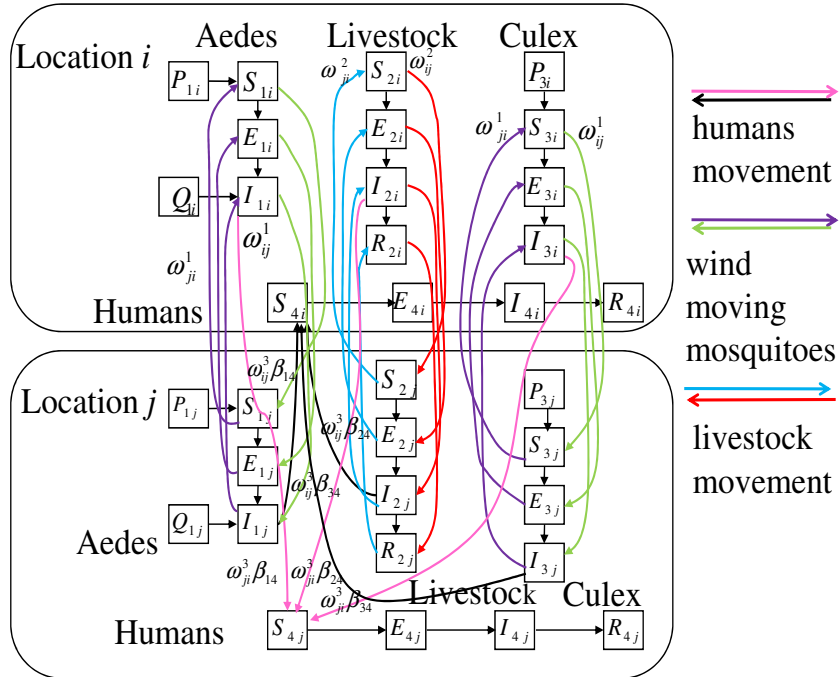
$$\frac{dS_{1i}}{dt} = \theta_1 P_{1i} + \sum_{j=1, j \neq i}^n \omega_{ji}^1 S_{1j} - \sum_{j=1, j \neq i}^n \omega_{ij}^1 S_{1i} - d_1 S_{1i} N_{1i} / K_1 - \beta_{21} S_{1i} I_{2i} / N_{2i} \quad (3)$$

$$\frac{dE_{1i}}{dt} = \sum_{j=1, j \neq i}^n \omega_{ji}^1 E_{1j} - \sum_{j=1, j \neq i}^n \omega_{ij}^1 E_{1i} - d_1 E_{1i} N_{1i} / K_1 + \beta_{21} S_{1i} I_{2i} / N_{2i} - \varepsilon_1 E_{1i} \quad (4)$$

$$\frac{dI_{1i}}{dt} = \sum_{j=1, j \neq i}^n \omega_{ji}^1 I_{1j} - \sum_{j=1, j \neq i}^n \omega_{ij}^1 I_{1i} + \theta_1 Q_{1i} - d_1 I_{1i} N_{1i} / K_1 + \varepsilon_1 E_{1i} \quad (5)$$



(a) Local transmission flow diagram of rift valley fever



(b) RVFv transmission between different locations

Figure 1: Flow diagram of RVF transmission

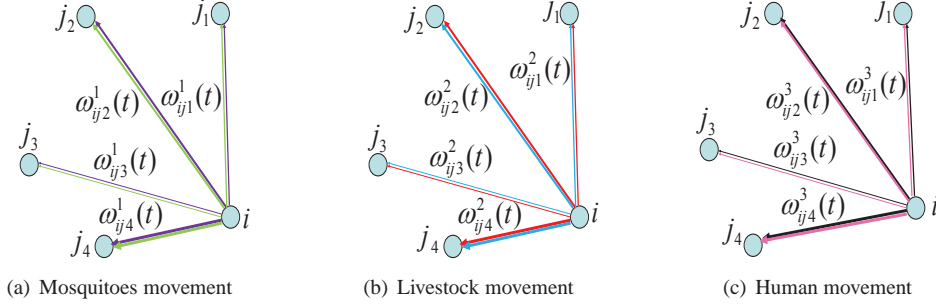


Figure 2: Network graphs of node  $i$  with links to generic neighbors (the same color code used in Figure 1 applies here)

$$\begin{aligned}
\frac{dN_{1i}}{dt} &= \theta_1(P_{1i} + Q_{1i}) + \sum_{j=1, j \neq i}^n \omega_{ji}^1 S_{1j} - \sum_{j=1, j \neq i}^n \omega_{ij}^1 S_{1i} + \sum_{j=1, j \neq i}^n \omega_{ji}^1 E_{1j} - \sum_{j=1, j \neq i}^n \omega_{ij}^1 E_{1i} \\
&+ \sum_{j=1, j \neq i}^n \omega_{ji}^1 I_{1j} - \sum_{j=1, j \neq i}^n \omega_{ij}^1 I_{1i} - d_1 S_{1i} N_{1i} / K_1
\end{aligned} \tag{6}$$

In reality, the above model is a modified ‘‘S-E-I’’ model since compartments P and Q are included in the model. Compartments P and Q represent uninfected eggs and infected eggs respectively. The number of infected humans and livestock readily increases in location  $i$  if we increase the number of uninfected or infected eggs. The total number of eggs laid each day is  $b_1 N_{1i}$ . The number of infected eggs laid each day is  $b_1 q_1 I_{1i}$ . So the number of uninfected eggs is  $b_1 N_{1i} - b_1 q_1 I_{1i}$ . The number of dead individuals in each compartment  $[m]$  for *Aedes* mosquitoes population is given as  $d_1 X_{1i}^{[m]} N_{1i} / K_1$ . We subtract dead individuals from the compartment they belong to since they are removed from the compartments. The change of the number of infected animals due to mobility in each compartment is given as  $\sum_{j=1, j \neq i}^n \omega_{ji}^1 X_{1j}^{[m]} - \sum_{j=1, j \neq i}^n \omega_{ij}^1 X_{1i}^{[m]}$  for *Aedes* mosquitoes. Obviously, if the number of mosquitoes in each compartment moving in is greater than for those moving out, the number of the mosquitoes in that compartment increases.  $\theta_1 P_{1i}$  is the number of uninfected eggs that develop into susceptible adult *Aedes* mosquitoes.  $\theta_1 Q_{1i}$  is the number of infected eggs that develop into infected adult *Aedes* mosquitoes. The infection of *Aedes* mosquitoes from livestock is denoted by  $\beta_{21} S_{1i} I_{2i} / N_{2i}$ . The number of infected *Aedes* mosquitoes increases and those susceptible decreases due to the infection. The number of infected *Aedes* mosquitoes increases when the infected eggs develop into adult *Aedes* mosquitoes. We represent the number of *Aedes* mosquitoes transferring from exposed state to infected state as  $\varepsilon_1 E_{1i}$ . The number of *Aedes* mosquitoes in the exposed state decreases and those in infected state increases after this transformation.

### 2.2.2. *Culex* mosquito vectors

$$\frac{dP_{3i}}{dt} = b_3(temp, t) N_{3i} - \theta_3(temp, t) P_{3i} \tag{7}$$

$$\frac{dS_{3i}}{dt} = \theta_3(temp, t) P_{3i} + \sum_{j=1, j \neq i}^n \omega_{ji}^1 S_{3j} - \sum_{j=1, j \neq i}^n \omega_{ij}^1 S_{3i} - d_3 S_{3i} N_{3i} / K_3 - \beta_{23} S_{3i} I_{2i} / N_{2i} \tag{8}$$

$$\frac{dE_{3i}}{dt} = \sum_{j=1, j \neq i}^n \omega_{ji}^1 E_{3j} - \sum_{j=1, j \neq i}^n \omega_{ij}^1 E_{3i} - \varepsilon_3 E_{3i} - d_3 E_{3i} N_{3i} / K_3 + \beta_{23} S_{3i} I_{2i} / N_{2i} \quad (9)$$

$$\frac{dI_{3i}}{dt} = \sum_{j=1, j \neq i}^n \omega_{ji}^1 I_{3j} - \sum_{j=1, j \neq i}^n \omega_{ij}^1 I_{3i} + \varepsilon_3 E_{3i} - d_3 I_{3i} N_{3i} / K_3 \quad (10)$$

$$\begin{aligned} \frac{dN_{3i}}{dt} &= \theta_3(temp, t) P_{3i} - d_3 N_{3i} N_{3i} / K_3 + \sum_{j=1, j \neq i}^n \omega_{ji}^1 S_{3j} - \sum_{j=1, j \neq i}^n \omega_{ij}^1 S_{3i} \\ &+ \sum_{j=1, j \neq i}^n \omega_{ji}^1 E_{3j} - \sum_{j=1, j \neq i}^n \omega_{ij}^1 E_{3i} + \sum_{j=1, j \neq i}^n \omega_{ji}^1 I_{3j} - \sum_{j=1, j \neq i}^n \omega_{ij}^1 I_{3i} \end{aligned} \quad (11)$$

We also use a modified ‘‘S-E-I’’ model for *Culex* mosquitoes. Compartment P represents uninfected eggs. Only uninfected eggs are included since the female *Culex* mosquito has not been demonstrated to transmit RVFv to its own eggs [20]. The number of infected humans and livestock increases in location  $i$  if we increase the number of uninfected or infected eggs. The total number of eggs laid each day is  $b_3(temp, t)N_{3i}$ . The number of dead individuals in each compartment  $[m]$  for *Culex* mosquitoes population is given as  $d_3 X_{3i}^{[m]} N_{3i} / K_3$  because they are removed from the compartments. So we subtract them from the compartment. The change of the number of infected *Culex* mosquitoes due to movement is given as  $\sum_{j=1, j \neq i}^n \omega_{ji}^1 X_{3j}^{[m]} - \sum_{j=1, j \neq i}^n \omega_{ij}^1 X_{3i}^{[m]}$  for *Culex* mosquitoes.  $\theta_3 P_{3i}$  is the number of uninfected eggs that develop into susceptible adult *Culex* mosquitoes. The number of susceptible *Culex* mosquitoes increases with the uninfected eggs developing into adult *Culex* mosquitoes. The infection of *Culex* mosquitoes from livestock is denoted by  $\beta_{23} S_{3i} I_{2i} / N_{2i}$ . The number of infected *Culex* mosquitoes increases while that of the susceptible *Culex* mosquitoes decreases due to the infection. We represent the number of *Culex* mosquitoes transferred from exposed state to infected state as  $\varepsilon_1 E_{3i}$ . The number of *Culex* mosquitoes in exposed state decreases and those in infected state increases after this transformation. The total number of *Culex* mosquitoes is also variable. It’s the sum of the *Culex* mosquitoes in all the compartments.

### 2.2.3. Livestock hosts

$$\begin{aligned} \frac{dS_{2i}}{dt} &= b_2 N_{2i} + \sum_{j=1, j \neq i}^n \omega_{ji}^2 S_{2j} - \sum_{j=1, j \neq i}^n \omega_{ij}^2 S_{2i} - d_2 S_{2i} N_{2i} / K_2 - \beta_{12} S_{2i} I_{1i} / N_{1i} \\ &- \beta_{32} S_{2i} I_{3i} / N_{3i} \end{aligned} \quad (12)$$

$$\begin{aligned} \frac{dE_{2i}}{dt} &= \sum_{j=1, j \neq i}^n \omega_{ji}^2 E_{2j} - \sum_{j=1, j \neq i}^n \omega_{ij}^2 E_{2i} - d_2 E_{2i} N_{2i} / K_2 - \varepsilon_2 E_{2i} + \beta_{12} S_{2i} I_{1i} / N_{1i} \\ &+ \beta_{32} S_{2i} I_{3i} / N_{3i} \end{aligned} \quad (13)$$

$$\frac{dI_{2i}}{dt} = \sum_{j=1, j \neq i}^n \omega_{ji}^2 I_{2j} - \sum_{j=1, j \neq i}^n \omega_{ij}^2 I_{2i} - d_2 I_{2i} N_{2i} / K_2 + \varepsilon_2 E_{2i} - \gamma_2 I_{2i} - \mu_2 I_{2i} \quad (14)$$

$$\frac{dR_{2i}}{dt} = \sum_{j=1, j \neq i}^n \omega_{ji}^2 R_{2j} - \sum_{j=1, j \neq i}^n \omega_{ij}^2 R_{2i} + \gamma_2 I_{2i} - d_2 R_{2i} N_{2i} / K_2 \quad (15)$$

$$\begin{aligned}
\frac{dN_{2i}}{dt} = & (b_2 - d_2 N_{2i}/K_2)N_{2i} - \mu_2 I_{2i} + \sum_{j=1, j \neq i}^n \omega_{ji}^2 S_{2j} - \sum_{j=1, j \neq i}^n \omega_{ij}^2 S_{2i} + \sum_{j=1, j \neq i}^n \omega_{ji}^2 E_{2j} \\
& - \sum_{j=1, j \neq i}^n \omega_{ij}^2 E_{2i} + \sum_{j=1, j \neq i}^n \omega_{ji}^2 I_{2j} - \sum_{j=1, j \neq i}^n \omega_{ij}^2 I_{2i} + \sum_{j=1, j \neq i}^n \omega_{ji}^2 R_{2j} - \sum_{j=1, j \neq i}^n \omega_{ij}^2 R_{2i} \quad (16)
\end{aligned}$$

Mitigation scenarios are not considered in our model. We assume infected animals might be transported to other provinces for trading, slaughtering, or other purposes even they are infectious. The total number of newborn livestock in location  $i$  is  $b_2 N_{2i}$  each day. The number of dead individuals in each compartment  $[m]$  for livestock population is given as  $d_2 X_{2i}^{[m]} N_{2i}/K_2$ . We subtract dead individuals from the compartment they belong to since they are removed from the compartments. So w. The change of the number of infected animals due to movement is given as  $\sum_{j=1, j \neq i}^n \omega_{ji}^2 X_{2j}^{[m]} - \sum_{j=1, j \neq i}^n \omega_{ij}^2 X_{2i}^{[m]}$  for livestock. Obviously, if the number of livestock in each compartment moving in is greater than those moving out, the number of livestock in that compartment increases. We represent the number of livestock that transfer from exposed state to infected state as  $\varepsilon_2 E_{2i}$ . The infection from *Aedes* mosquitoes and *Culex* mosquitoes are denoted as  $\beta_{12} S_{2i} I_{1i}/N_{1i}$  and  $\beta_{32} S_{2i} I_{3i}/N_{3i}$  respectively. The number of livestock in exposed state decreases and those in infected state increases after this transformation. The number of recovered livestock is  $\gamma_2 I_{2i}$ . The number of livestock die of RVF is  $\mu_2 I_{2i}$ .

#### 2.2.4. Human hosts

$$\begin{aligned}
\frac{dS_{4i}}{dt} = & b_4 N_{4i} - d_4 S_{4i} N_{4i}/K_4 - \frac{\beta_{14} S_{4i} I_{1i}/N_{1i}}{1 + \sigma_i/\tau} - \frac{\beta_{24} f_i S_{4i} I_{2i}/N_{2i}}{1 + \sigma_i/\tau} - \frac{\beta_{34} S_{4i} I_{3i}/N_{3i}}{1 + \sigma_i/\tau} \\
& - \sum_{j=1, j \neq i}^n \frac{\beta_{14} S_{4i} I_{1j}/N_{1j} \sigma_{ij}/\tau}{1 + \sigma_i/\tau} - \sum_{j=1, j \neq i}^n \frac{\beta_{24} f_i S_{4i} I_{2j}/N_{2j} \sigma_{ij}/\tau}{1 + \sigma_i/\tau} - \sum_{j=1, j \neq i}^n \frac{\beta_{34} S_{4i} I_{3j}/N_{3j} \sigma_{ij}/\tau}{1 + \sigma_i/\tau} [47] \quad (17)
\end{aligned}$$

$$\begin{aligned}
\frac{dE_{4i}}{dt} = & \frac{\beta_{14} S_{4i} I_{1i}/N_{1i}}{1 + \sigma_i/\tau} + \frac{\beta_{24} f_i S_{4i} I_{2i}/N_{2i}}{1 + \sigma_i/\tau} + \frac{\beta_{34} S_{4i} I_{3i}/N_{3i}}{1 + \sigma_i/\tau} + \sum_{j=1}^n \frac{\beta_{14} S_{4i} I_{1j}/N_{1j} \sigma_{ij}/\tau}{1 + \sigma_i/\tau} \\
& + \sum_{j=1}^n \frac{\beta_{24} f_i S_{4i} I_{2j}/N_{2j} \sigma_{ij}/\tau}{1 + \sigma_i/\tau} + \sum_{j=1}^n \frac{\beta_{34} S_{4i} I_{3j}/N_{3j} \sigma_{ij}/\tau}{1 + \sigma_i/\tau} - d_4 E_{4i} N_{4i}/K_4 - \varepsilon_4 E_{4i} [47] \quad (18)
\end{aligned}$$

$$\frac{dI_{4i}}{dt} = -d_4 I_{4i} N_{4i}/K_4 + \varepsilon_4 E_{4i} - \gamma_4 I_{4i} - \mu_4 I_{4i} \quad (19)$$

$$\frac{dR_{4i}}{dt} = \gamma_4 I_{4i} - d_4 R_{4i} N_{4i}/K_4 \quad (20)$$

$$\frac{dN_{4i}}{dt} = (b_4 - d_4 N_{4i}/K_4) N_{4i} - \mu_4 I_{4i} \quad (21)$$

The contact rate from livestock to humans is much higher than other contact rates. We assume susceptible human population only includes those working with animals such as veterinarians and farmers since they are at higher risk of RVFv infection [15]. The total number of newborn humans in location  $i$  is  $b_4 N_{4i}$  each day. The number of dead individuals in each compartment

$[m]$  for human population is given as  $d_4 X_{4i}^{[m]} N_{4i} / K_4$  because they are removed from the compartments. So we subtract them from the compartment. Obviously, if the number of humans in each compartment moving in is greater than those moving out, the number of the humans in that compartment increases. Humans might acquire the infection from *Aedes* mosquitoes, *Culex* mosquitoes, and livestock. We represent the number of humans that transfer from exposed state to infected state as  $\varepsilon_4 E_{4i}$ . The number of humans in exposed state decreases and those in infected state increases after this transformation. The number of recovered humans is  $\gamma_4 I_{4i}$ . The number of humans dying of RVF is  $\mu_4 I_{4i}$ .

### 2.2.5. Model Parameters

The equation (22) is used to model the development rate of *Culex* mosquitoes [21]. The daily egg laying rate expressed in equation (24) is a function of moisture [21]. Moisture in equation (23) is obtained by summing the difference of precipitation [11] and evaporation (mm) [27] over the proceeding 7 days [21]. In the equations (22) to (24), A, HA, HH, K, TH, Emax, Evar, Emean, BaselineEggrate are parameters [21]. The parameter description and values are shown in Table 1.

$$\theta_3(temp, t) = A * \frac{(Temperature(t) + K)}{298.15} * \frac{\exp[\frac{HA}{1.987} * (\frac{1}{298.15} - \frac{1}{Temperature(t)+K})]}{1 + \exp[\frac{HH}{1.987} * (\frac{1}{TH} - \frac{1}{Temperature(t)+K})]} \quad (22)$$

$$Moisture(t) = \sum_{D=t-6}^t participation(D) - evaporation(D) \quad (23)$$

$$b_3(temp, precipitation, t) = BaselineEggrate + \frac{Emax}{1 + \exp[-\frac{Moisture(t)-Emean}{Evar}]} \quad (24)$$

### 2.2.6. Network Weights

The superscripts of  $\omega_{ij}$  in the equations (25) to (27) mean the movement of different species. The number 1 means movement of *Aedes* or *Culex* population, 2 means livestock movement, and 3 means human movement. The subscript  $ij$  of  $\omega_{ij}$  means the direction of the movement is from location  $i$  to location  $j$ . The weighted network graph is depicted in Figure 2. The difference in the thickness of the lines represent the difference in weight. Thicker lines represents larger weight. The weight for each population is between 0 and 1. We parameterize the weight due to mosquito movement with wind [25, 13], livestock movement due to transportation to feedlots or trade centers, and human mobility due to commuting as shown in equations 27 to 29 [21]. We use the wind data [34] in Bloemfontein, which is the capital of Free State, as the wind of Free State Province, that of Kimberley, which is the capital of Northern Cape, as the wind of Northern Cape Province and that of Grahams town, which is the center of Eastern Cape province, as the wind of Eastern Cape province. The distance vector is calculated with longitude and latitude in each location. Livestock population [4], the number of animals sold [1], the number of animals in the feedlots [31] are factors of weight for livestock movement. Distance and human population [3] affect the weight for human movement. Weight for mosquito movement is decided by the projection of wind in the direction of distance vector [13]. The income from animals is considered in the weight for animal movement.

$$\omega_{ij}^1 = c_1 \frac{\vec{W}_i \cdot \vec{D}_{ij}}{|\vec{D}_{ij}|} \frac{1}{|\vec{D}_{ij}|} \quad (25)$$

Parameter	Description	Value	Units	Reference
$\beta_{12}$	adequate contact rate: <i>Aedes</i> to livestock	0.002	1/day	[20]
$\beta_{21}$	adequate contact rate: livestock to <i>Aedes</i>	0.0021	1/day	[20]
$\beta_{23}$	adequate contact rate: livestock to <i>Culex</i>	0.000001	1/day	[20]
$\beta_{32}$	adequate contact rate: <i>Culex</i> to livestock	0.00001	1/day	[20]
$\beta_{14}$	adequate contact rate: <i>Aedes</i> to humans	0.000006	1/day	
$\beta_{24}$	adequate contact rate: livestock to humans	0.00017	1/day	
$\beta_{34}$	adequate contact rate: <i>Culex</i> to humans	0.0000001	1/day	
$\gamma_2$	recover rate in livestock	0.14	1/day	[20]
$\gamma_4$	recover rate in humans	0.14	1/day	[3, 2, 1]
$d_1$	death rate of <i>Aedes</i> mosquitoes	0.025	1/day	[20]
$d_2$	death rate of livestock	1/3650	1/day	[20]
$d_3$	death rate of <i>Culex</i> mosquitoes	1/40	1/day	[20]
$d_4$	death rate of humans	1/18615	1/day	[3, 2, 1]
$b_1$	number of <i>Aedes</i> eggs laid per day	0.05	1/day	[20]
$b_2$	daily birthrate of livestock	0.0028	1/day	[20]
$b_3$	number of <i>Culex</i> eggs laid per day		1/day	[21]
$b_4$	daily birthrate of humans	1/14600	1/day	[3, 2, 1]
$1/\epsilon_1$	incubation period in <i>Aedes</i> mosquitoes	6	days	[20]
$1/\epsilon_2$	incubation period in livestock	4	days	[20]
$1/\epsilon_3$	incubation period in <i>Culex</i> mosquitoes	6	days	[20]
$1/\epsilon_4$	incubation period in humans	4	days	[32]
$\mu_2$	mortality rate in sheep	0.0312	-	[20]
$\mu_4$	mortality rate in humans	0.0001	1/day	[3, 2, 1]
$q_1$	transovarial transmission rate in livestock	0.05	-	[20]
$1/\theta_1$	development time of <i>Aedes</i>	15	days	[20]
$\theta_3$	development rate of <i>Culex</i>		1/day	[21]
$A$	parameter of the development rate	0.25		[21]
$HA$	parameter of the development rate	28094		[21]
$HH$	parameter of the development rate	35692	1/day	[21]
$TH$	parameter of the development rate function	298.6	1/day	[21]
<i>BaselineEggrate</i>	minimum constant fecundity rate	3	1/day	[21]
<i>E<sub>max</sub></i>	maximum daily egg laying rate	3	1/day	[21]
<i>E<sub>mean</sub></i>	the mean of the daily egg laying rate	0	1/day	[21]]
$1/Evar$	the variance of the daily egg laying rate	12	1/day	[21]
$K_1$	carrying capacity of <i>Aedes</i> mosquitoes	1000000000	-	
$K_2$	carrying capacity of livestock	10000000	-	
$K_3$	carrying capacity of <i>Culex</i> mosquitoes	1000000000	-	
$K_4$	carrying capacity of humans	10000000	-	
$K$	Kelvin parameter	273.15	Kelvin	[21]
$f_i$	fraction of those working with animals	0.82	1/day	[15]
$\tau$	return rate	3	-	[15]

Table 1: Parameter values for numerical simulation

$$\omega_{ij}^2 = c_2 \frac{FM_j}{FM_i} \frac{1}{|\vec{D}_{ij}|} \quad (26)$$

$$\omega_{ij}^3 = c_3 \frac{N_i^\alpha N_j^\gamma}{e^{\beta|\vec{D}_{ij}|}} \quad (27)$$

$$\sigma_{ij} = \frac{\omega_{ij}^3}{N_i} \quad (28)$$

$$\sigma_i = \sum_{j=1, j \neq i}^n \frac{\omega_{ij}^3}{N_i} \quad (29)$$

Here:

$\vec{W}_i$  = the wind vector in location  $i$  [13]

$\vec{D}_{ij}$  = the distance vector from location  $i$  to location  $j$

$\omega_{ij}^1(t)$  = the weight for mosquitoes moving from location  $i$  to location  $j$

$\omega_{ij}^2(t)$  = the weight for livestock moving from location  $i$  to location  $j$

$\omega_{ij}^3(t)$  = the number of commuters between location  $i$  and location  $j$

$FM_i$  = number of animals in markets and feedlots  $i$

$N_i$  = the number of humans in location  $i$  [3]

$\sigma_{ij}$  the commuting rate between subpopulation  $i$  and each of its neighbor  $j$  [9]

$\sigma_i$  daily total rate of commuting for the population  $i$  [9]

### 3. Case Study: South Africa 2010

We have used data from the South African RVF outbreak in 2010 as a case study. Outbreak data for animals are obtained from [10, 16], while outbreak data for human subpopulations were collected from [4, 15]. As far as animal data is concerned, we chose to analyze RVF incidence in the sheep population. Since the granularity of human incidence data is provided at the Province level, each node in the network represents a province. We selected three provinces: Free State (location 1), Northern Cape (location 2) and Eastern Cape (location 3), since they had the highest levels of RVF incidence for humans. The curves of the incidence data are shown in Figure 3 using green histograms, while the red curves represent simulations obtained with our model. From the data in Figure 3, it is possible to observe that the epidemic started first in the Free State Province and later in Northern Cape. This is due to the fact that the sustained heavy rainfall, which triggered the outbreak, started later in Northern Cape, causing infected eggs hatching later than those in the Free State Province. Additionally, it is evident that number of animal and human cases in Eastern Cape is smaller than the other two provinces, while Free State is the most affected node.

To explore the behavior of RVF, we conducted numerical simulations of an open system considering movement of the four species among different locations. To test the validity of our model, we changed some parameters in the weights to see the impact of those variations. If  $Q_{11} = 10$ ,  $Q_{12} = 0$ ,  $Q_{13} = 0$ , at the beginning infected eggs only exist in location 1, Free State. However, our model considers movement of mosquitoes to other locations with wind. As a consequence, infected animals and humans appear in all three locations as is shown in Figure 4. So the infection spreads due to movement of the four populations. If we also assume that at

the beginning infected eggs only exist in location 1,  $Q_{11} = 10$ ,  $Q_{12} = 0$ ,  $Q_{13} = 0$ , and movements of the four species from one location to another are not allowed,  $c_1 = 0$ ,  $c_2 = 0$ ,  $c_3 = 0$ , then infected animals and humans dont appear in location 2 and location 3 as it is shown in Figure 5. We can test the mitigation strategy of movement ban with this model.

#### 4. Sensitivity analysis

The three parameters  $c_1$ ,  $c_2$  and  $c_3$  are estimated using the least square approach, which is based on minimization of errors between the incidence data of livestock and humans and the percentage of infected livestock or humans calculated by the mathematical model. At first, we establish an objective function. Since the weight for each population is in the range  $[0, 1]$  as mentioned above, so there is lower bound and upper bound for parameters  $c_1$ ,  $c_2$  and  $c_3$ . At each sample time, we calculate the difference of the prevalence of livestock calculated by differential equations and that reported by [10], and the difference of the number of humans calculated by differential equations and that reported [24] during outbreaks in three provinces of South Africa from January, 2010. We calculate the square of each difference. Then we add all the squares for each location in each day together to obtain the objective function as is shown below. Minimization of the objective function is initiated by providing initial guesses  $c_{10}$ ,  $c_{20}$  and  $c_{30}$  for each parameter. The differential equations are solved with each set of the parameters and the square errors between the number of infected humans obtained from the objective function and those from incidence data are calculated. The set of parameters corresponding to the minimum value for the objective function is the set of optimal parameters listed in Table 2.

$$F = \sum_{t=t_0}^{t_f} \sum_{i=1}^n [(I_{4i}(t) - PR_{4i}(t))^2] \quad (30)$$

In the equations above,  $n$  = the number of nodes

$t_0$  =starting time

$t_f$  =end time

$I_{4i}(t)$  =human prevalence calculated by the model

$PR_{4i}(t)$  =human prevalence by time  $t$

To conduct a sensitivity analysis of the parameters  $c_1$ ,  $c_2$ ,  $c_3$  of the model, we have changed each parameter within  $\pm 10\%$  of the optimized value, keeping the other parameters constant. This analysis allows an evaluation of the impact of uncertainties in the parameter estimations. The relative errors between the fractions of infected humans are calculated for each set of parameters, in each location, at time  $t$  as  $|\frac{I_{4i}(t) - PR_{4i}(t)}{I_{4i}(t)}|$ . The relative errors are shown in Table 3, using the following notation:

$e_{1h}$  =relative error of human incidence with  $c_2$ ,  $c_3$  fixed

$e_{2h}$  =relative error of human incidence with  $c_1$ ,  $c_3$  fixed

$e_{3h}$  =relative error of human incidence with  $c_1$ ,  $c_2$  fixed

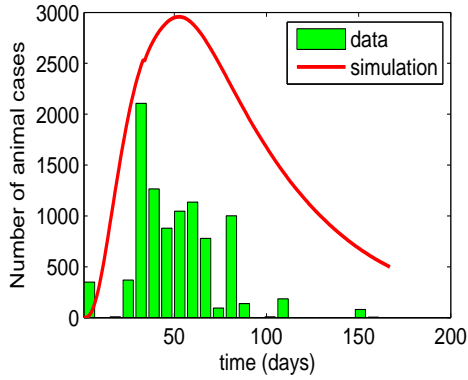
All the values of relative errors shown in Table 3 are smaller than 10%, proving the model robustness with respect to limited uncertainties in the parameter estimation.

$c_1$	$c_2$	$c_3$
0.009	0.05	0.005

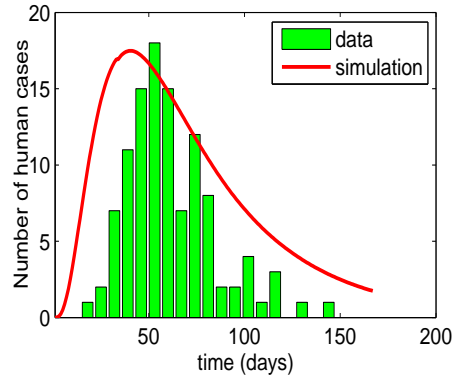
Table 2: Optimized model parameters

$e_{1h}$	$e_{2h}$	$e_{3h}$
0.033868	0.086998	0.00354
0.032435	0.077771	0.003186
0.018287	0.062683	0.002832
0.028099	0.05523	0.002478
0.029105	0.055105	0.002124
0.033749	0.034578	0.00177
0.014393	0.030048	0.001416
0.021108	0.021863	0.001062
0.012957	0.017858	0.000708
0.006633	0.007078	0.000354
0	0	0
0.010479	0.00778	0.000354
0.015346	0.019272	0.000708
0.008848	0.026241	0.001062
0.024176	0.035252	0.001416
0.010849	0.04696	0.00177
0.015531	0.061346	0.002124
0.021478	0.060327	0.002478
0.015362	0.080435	0.002832
0.014702	0.079326	0.003186
0.021724	0.083646	0.00354
0.01853	0.045228	0.001854

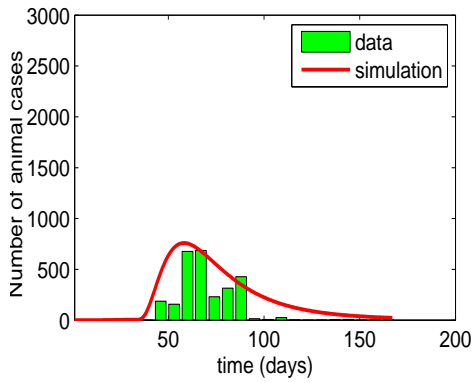
Table 3: Relative error of livestock and human prevalence with different parameters



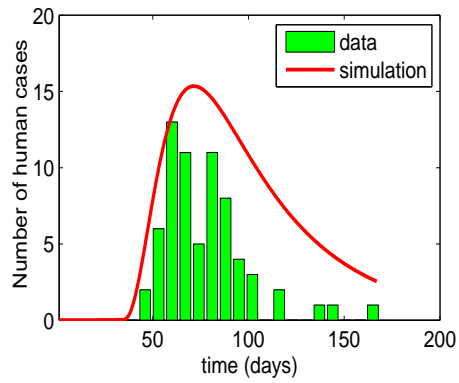
(a) Simulation result and incidence data for sheep in Free State Province



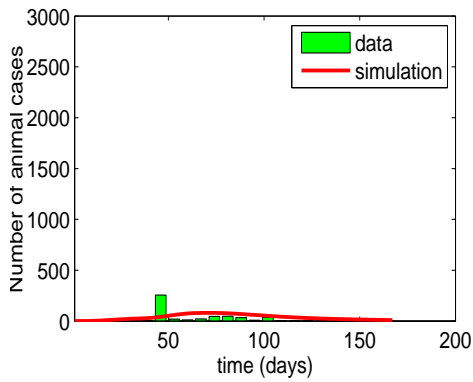
(b) Simulation result and incidence data for humans in Free State Province



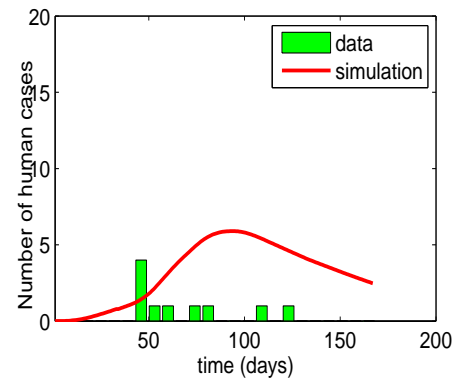
(c) Simulation result and incidence data for sheep in Northern Cape Province



(d) Simulation result and incidence data for humans in Northern Cape Province



(e) Simulation result and incidence data for sheep in Eastern Cape Province



(f) Simulation result and incidence data for humans in Eastern Cape Province

Figure 3: Simulation results and incidence data in South Africa

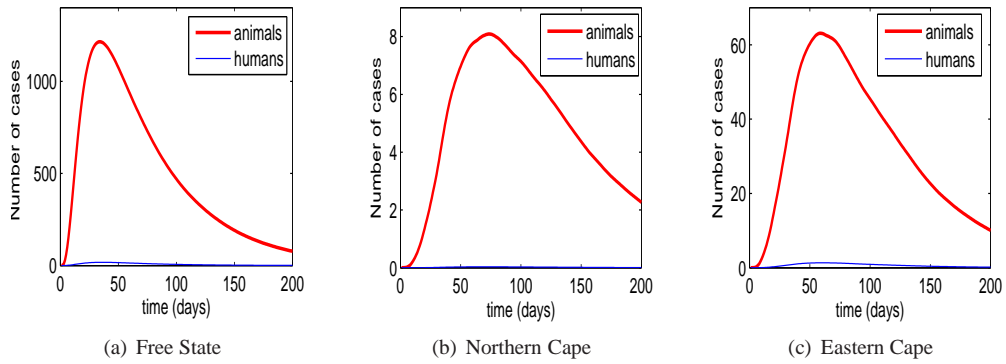


Figure 4: Simulation results with  $c_1 \neq 0$

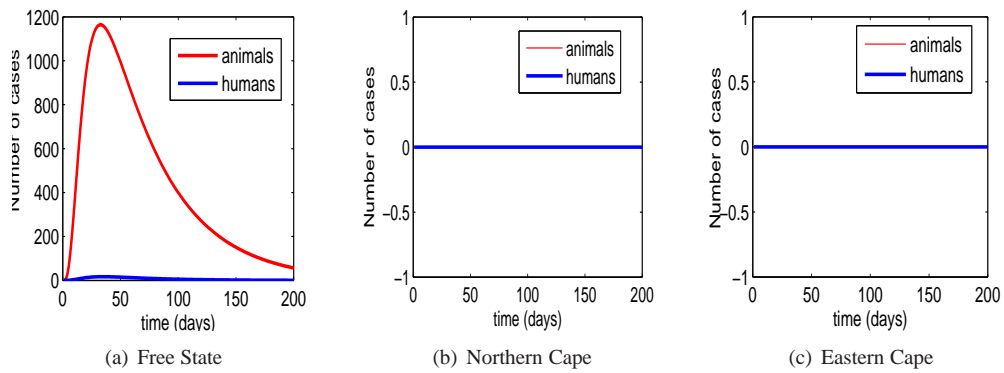


Figure 5: Simulation results with  $c_1 = c_2 = c_3 = 0$

## 5. Analysis of Simulation Results

Using the computed optimal parameters, we performed the simulations to reproduce the RVF outbreak in the three South African Provinces considered. The simulation results are shown in Figure 3. Not only our model can differentiate the maximum number of infected individuals among the three different provinces, but also could reproduce the different starting times of the outbreak in the three locations. Obviously, with a homogeneous population model, such as the one in [20], the spatial differentiation is not possible.

We imposed that the animal incidence curves provided by the model were always an over-estimation of the data, since underreporting is very common in this case. Finally, our approach in which the fractions of each subpopulation in each compartment are expressed as continuous variables, require a large number of cases to be accurate. For this reason, the incidence data for location 3, Eastern Cape, would better be approximated by a stochastic model.

If our model is simulated for a longer scale, there will be reappearances of Rift Valley Fever, as it is shown in Figure 6. Due to the flexibility and accuracy of our proposed model, we can test and design multiple and different mitigation strategies in different locations at different time.

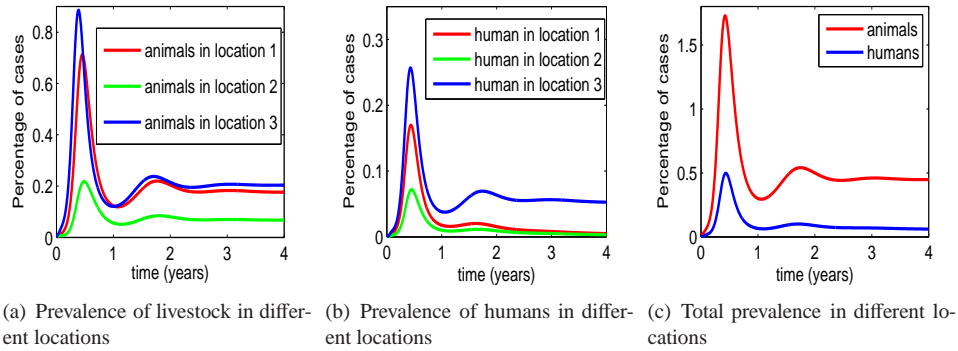


Figure 6: Simulation of generic infection network

## 6. Conclusions and discussions

We characterize a meta-population, network-based, deterministic RVF model that predicts the spatial-temporal epidemic spread. When considering  $n$  locations or nodes ( $n \geq 1$ ), there are  $21 * n$  differential equations and  $21 * n$  variables in our model, while there are only 16 equations with 16 variables in the model presented in [20]. Obviously, greater accuracy of our model is obtained at the cost of an increased complexity. The novelty of our model is that it considers a weighted contact network to represent the movement of four species, including humans who were not considered in [20]. Subpopulations at the node level are also incorporated in our model. The model has been evaluated using data from the recent outbreak in South Africa, and has shown to be very promising notwithstanding the limitation of the data.

Future work in follow-up mathematical models includes the development of a stochastic model, the study of the impact of climate changes on the epidemiology and control of Rift Valley Fever, and the improvement of the wind model considering diffusion equations. Moreover, the

time for travel as a delay function will be incorporated in the model, and carrying capacities will be considered dependent on climate factors in the future.

## Acknowledgments

This work has been supported by the National Agricultural Biosecurity Center (NABC) at Kansas State University, and by the DHS Center of Excellence for Emerging and Zoonotic Animal Diseases (CEEZAD). We are grateful to Jason Coleman, Regina M. Beard, and Kelebogile Olifant for their help on bibliography research. We would also like to give thanks to Duygu Balcan, Anton Lyubinin, and Getahun Agga for the comments on the paper, and Kristine Bennett for answering questions on entomology.

## References

- [1] Africa, S.S., Accessed Nov 22, 2010a. Agricultural census (census of commercial agriculture), 2007. <http://www.statssa.gov.za/publications/statsdownload.asp?PPN=P1102&SCH=4534>.
- [2] Africa, S.S., Accessed Nov 22, 2010b. Domestic tourism survey 2009. <http://www.statsonline.gov.za/publications/statsdownload.asp?PPN=P0352.1&SCH=4702>.
- [3] Africa, S.S., Accessed Nov 22, 2010c. Mid-year population estimates. <http://www.statsonline.gov.za/publications/P0302/P03022010.pdf>.
- [4] Department of Agriculture, F., of Republic of South Africa, F., Accessed Sep 26, 2010. Livestock number 96 to date. <http://www.nda.agric.za/docs/statsinfo/LivestokNo96toDate.xls>.
- [5] Anyamba, A., Chretien, J.P., Small, J., Tucker, C.J., Formenty, P.B., Richardson, J.H., Britch, S.C., Schnabel, D.C., Erickson, R.L., Linthicum, K.J., 2009. Prediction of a rift valley fever outbreak. *Proceedings of the National Academy of Sciences* 106, 955–959.
- [6] Anyamba, A., Chretien, J.P., Small, J., Tucker, C.J., Linthicum, K.J., 2006. Developing global climate anomalies suggest potential disease risks for 2006–2007. *International journal of health geographics* 5, 60.
- [7] Anyamba, A., Linthicum, K.J., Mahoney, R., Tucker, C.J., 2002. Mapping potential risk of rift valley fever outbreaks in african savannas using vegetation index time series data. *Photogrammetric engineering and remote sensing* 68, 137–145.
- [8] Anyamba, A., Linthicum, K.J., Tucker, C.J., 2001. Climate-disease connections: Rift valley fever in kenya. *Cadernos de saude publica / Ministerio da Saude, Fundacao Oswaldo Cruz, Escola Nacional de Saude Publica* 17 Suppl, 133–140.
- [9] Balcan, D., Colizza, V., Goncalves, B., Hu, H., Ramasco, J.J., Vespignani, A., 2009. Multiscale mobility networks and the spatial spreading of infectious diseases. *Proceedings of the National Academy of Sciences of the United States of America* 106, 21484–21489.
- [10] BioPortal, D., Accessed Nov 23, 2010. <http://fmdbioportal.ucdavis.edu/about>.
- [11] center, N.C., Accessed Nov 22, 2010. Noaa satellite and information service. <http://www7.ncdc.noaa.gov/CD0/country>.
- [12] Chevalier, V., Lancelot, R., Thiongane, Y., Sall, B., Diaite, A., Mondet, B., 2005. Rift valley fever in small ruminants, senegal, 2003. *Emerging infectious diseases* 11, 1693–1700.
- [13] Chowdhury, S.R., Scoglio, C., Hsu, W., 2010. Simulative modeling to control the foot and mouth disease epidemic, in: *International Conference on Computational Science*, pp. 2261–2270.
- [14] Clements, A.C., Pfeiffer, D.U., Martin, V., Pittiglio, C., Best, N., Thiongane, Y., 2007. Spatial risk assessment of rift valley fever in senegal. *Vector borne and zoonotic diseases (Larchmont, N.Y.)* 7, 203–216.
- [15] for Communicable Diseases, N.I., Accessed Nov 23, 2010. Interim report on the rift valley fever (rvf) outbreak in south africa. [http://www.nicd.ac.za/outbreaks/rvf/docs/RVF\\_Interim\\_Report\\_2010\\_10\\_01.pdf](http://www.nicd.ac.za/outbreaks/rvf/docs/RVF_Interim_Report_2010_10_01.pdf).
- [16] Database, W.A.H.I., 2010. Summary of immediate notifications and follow-ups - 2010.
- [17] Davies, F.G., Martin, V., 2006. Recognizing rift valley fever. *Veterinaria italiana* 42, 31–53. JID: 0201543; ppublish.
- [18] for Disease Control, C., (CDC), P., 2007. Rift valley fever outbreak—kenya, november 2006–january 2007. *MMWR.Morbidity and mortality weekly report* 56, 73–76.
- [19] for Environment Food, D., Affairs, R., Accessed Nov 10, 2010. Rift valley fever. <http://www.defra.gov.uk/foodfarm/farmanimal/diseases/atoz/riftvalleyfever/index.htm>.

- [20] Gaff, H.D., Hartley, D.M., Leahy, N.P., 2007. An epidemiological model of rift valley fever. *Electron. J. Diff. Eqns* 2007, 1–12.
- [21] Gong, H., Degaetano, A.T., Harrington, L.C., 2010. Climate-based models for west nile culex mosquito vectors in the northeastern us. *International journal of biometeorology* .
- [22] Gubler, D.J., 2002. The global emergence/resurgence of arboviral diseases as public health problems. *Archives of Medical Research* 33, 330–342.
- [23] of Health, F.D., Accessed Nov 30, 2010a. Rift valley fever. <http://www.doh.state.fl.us/environment/medicine/arboviral/RiftValley>
- [24] of Health, S.A.D., Accessed Nov 30, 2010b. Press releases 2010. <http://www.doh.gov.za/docs/pr/>.
- [25] Kasari, T.R., Carr, D.A., Lynn, T.V., Weaver, J.T., 2008. Evaluation of pathways for release of rift valley fever virus into domestic ruminant livestock, ruminant wildlife, and human populations in the continental united states. *Journal of the American Veterinary Medical Association* 232, 514–529.
- [26] Konrad, S.K., s. N. Miller, Reeves, W.K., 2010. A spatially explicit degree-day model of rift valley fever transmission risk in the continental united states. *GeoJournal* .
- [27] Linacre, E.T., 1977. A simple formula for estimating evaporation rates in various climates using temperature data alone. *Agricultural Meteorology* 18, 409–424.
- [28] Linthicum, K.J., Anyamba, A., Britch, S.C., Chretien, J.P., Erickson, R.L., Small, J., Tucker, C.J., Bennett, K.E., Mayer, R.T., Schmidtman, E.T., Andreadis, T.G., Anderson, J.F., Wilson, W.C., Freier, J.E., James, A.M., Miller, R.S., Drolet, B.S., Miller, S.N., Tedrow, C.A., Bailey, C.L., Strickman, D.A., Barnard, D.R., Clark, G.G., Zou, L., 2007. A rift valley fever risk surveillance system for africa using remotely sensed data: potential for use on other continents. *Veterinaria italiana* 43, 663–674.
- [29] Linthicum, K.J., Davies, F.G., Kairo, A., Bailey, C.L., 1985. Rift valley fever virus (family bunyaviridae, genus phlebovirus). isolations from diptera collected during an inter-epizootic period in kenya. *The Journal of hygiene* 95, 197–209.
- [30] Martin, V., Chevalier, V., Ceccato, P., Anyamba, A., Simone, L.D., Lubroth, J., de La Rocque, S., Domenech, J., 2008. The impact of climate change on the epidemiology and control of rift valley fever. *Revue scientifique et technique (International Office of Epizootics)* 27, 413–426.
- [31] Olivier.C.G, Nov, 2004. An analysis of the south african beef supply chain: from farm to folk. url-<http://ujdigispace.uj.ac.za:8080/dspace/retrieve/1442/license.txt>.
- [32] Organization, W.H., Accessed Nov 22, 2010. Rift valley fever. <http://www.who.int/mediacentre/factsheets/fs207/en/>.
- [33] Sellers, R.F., Pedgley, D.E., Tucker, M.R., 1982. Rift valley fever, egypt 1977: disease spread by windborne insect vectors? *The Veterinary record* 110, 73–77.
- [34] Underground, W., Accessed Nov 20, 2010. Weather underground. <http://www.wunderground.com/>.
- [35] Woods, C.W., Karpati, A.M., Grein, T., McCarthy, N., Gaturuku, P., Muchiri, E., Dunster, L., Henderson, A., Khan, A.S., Swanepoel, R., Bonmarin, I., Martin, L., Mann, P., Smoak, B.L., Ryan, M., Ksiazek, T.G., Arthur, R.R., Ndikuyezze, A., Agata, N.N., Peters, C.J., Force, W.H.O.H.F.T., 2002. An outbreak of rift valley fever in northeastern kenya, 1997-98. *Emerging infectious diseases* 8, 138–144.
- [36] Zeller, H.G., Fontenille, D., Traore-Lamizana, M., Thiongane, Y., Digoutte, J.P., 1997. Enzootic activity of rift valley fever virus in senegal. *The American Journal of Tropical Medicine and Hygiene* 56, 265–272.